Materials Today Physics 8 (2019) 78–85

Contents lists available at ScienceDirect

Materials Today Physics

journal homepage: https://www.journals.elsevier.com/materials-today-physics

Ionic liquid–activated wearable electronics

J. Yang [a, b, 1], Q. Liu [a, c, 1], Z. Deng [a], M. Gong [a], F. Lei [a], J. Zhang [a, d], X. Zhang [b], Q. Wang [c], Y. Liu [e], Z. Wu [a, f], C.F. Guo [a, *]

[a] Department of Materials Science and Engineering & Shenzhen Engineering Research Center for Novel Electronic Information Materials and Devices, Southern University of Science and Technology, Shenzhen 518055, China
[b] School of Physics and TEDA Institute of Applied Physics, Nankai University, Tianjin, China
[c] Department of Mechanics and Aerospace Engineering, Southern University of Science and Technology, Shenzhen, China
[d] Academy for Advanced Interdisciplinary Studies, Southern University of Science and Technology, Shenzhen, China
[e] Department of Physics and TcSUH, University of Houston, Houston, TX, United States
[f] State Key Laboratory of Digital Manufacturing Equipment and Technology, Huazhong University of Science and Technology, Wuhan, China

ARTICLE INFO

Article history:
Received 30 January 2019
Received in revised form
12 February 2019
Accepted 12 February 2019
Available online 20 February 2019

Keywords:
Porous structure
Ionic liquid activation
Comfortable wearing interface
Human physiology signal and motion detection

ABSTRACT

Wearable electronics have been attracting increasing attention because of the potential applications in health care and body motion monitoring. However, the existing wearable electronic devices often appear as an extra part of clothing and show limited compatibility with various textiles. Here, we report a general, low-cost, and easy operating approach to fabricate wearable sensors based on commercial or synthesized textiles, for which the textile itself is the active material for sensing, by loading with an ionic liquid on the fabric skeleton followed by depositing flexible electrodes. This is a general method that can activate many other daily used porous materials for sensing applications. Here, the textile or porous materials act as the elastic framework that allows for fast response (tens of milliseconds), whereas the ionic liquid plays the role of an active material to achieve high sensitivity (up to 10 kPa^{-1}). The ionic liquid–activated wearable sensor allows for accurate monitoring of breathing, pulse wave, motion of the human joints, and plantar pressure. For clothing purpose, the sensor can be breathable, waterproof, washable, and antibacterial. This work provides a general strategy to make high-performance wearable electronics at low cost for health monitoring and motion detection.

1. Introduction

Cloth has evolved throughout human history, primarily for providing warmth for body and appearance purpose [1]. Very recently, cloth has been considered as a promising platform to incorporate into wearable electronics to monitor human activities through its intimate skin contact [2]. The most ideal form of wearable electronics is that the textile itself can function as a sensor—cloth worn on body measures motion and physiological signals when needed. A few wearable devices have been used to improve the health quality of humans or athletes' personal performance by offering precise health tracking and motion detection [3,4]. However, commercialized wearable electronics or those developed in laboratories typically consist of thin films or layered systems that are not compatible with textiles. Such devices often appear as a separate package or a unit that appears as wearable bands, smart watches, snaps, or sensing modules built in or on the surface of clothes. It is, therefore, significant to explore sensitive textiles or to activate common textiles that can replace the extra sensing modules on commercial cloth, thus achieving a comfortable wearing interface when tracking human motion and health.

In addition, high sensitivity of the sensing unit is necessary to monitor health and body motions precisely. Capacitive sensors have been widely developed in recent years because of the advantages such as fast response, low signal drift, and low energy consumption [5,6] compared with the piezoelectric [7–9] and resistive [10–12] sensors. Typically, the sensitivity and sensing range of the capacitive sensors mainly lie in the change of the distance between the plates. Although fabricating microstructured or porous dielectric layer is a way to offer sensors with diverse interfacial gaps to improve the sensitivity and response speed [13], the improvement is limited because of the limited change in geometry. Recently, an all-fabric supercapacitive pressure sensing

* Corresponding author.
E-mail address: guocf@sustc.edu.cn (C.F. Guo).
[1] Junlong Yang and Qingxian Liu contributed equally to this work.

https://doi.org/10.1016/j.mtphys.2019.02.002
2542-5293/

device was fabricated by sandwiching electrospun ionic nanofibers with two textile-like electrodes, achieving an ultrahigh capacitance to a pressure sensitivity of 114 nF kPa^{-1} [14]. Such an ionic dielectric exhibited a far larger specific capacitance than conventional direct capacitive sensors because of the formation of an electric double layer (EDL) for which the charges of different signs are at a nanoscale distance [15,16]. However, the electrospun ionic nanofiber layer is usually poor in mechanical strength, thus not being compatible with commercial textiles and large-scale fabrication for clothing purpose. By contrast, fabric textiles seem to be suitable for the wearable electronics because of the features such as light weight, flexibility, and inherent warm and snug properties [17–19]. A technique that is able to activate commercial textiles or to make active textiles for robust and highly sensitive textile-like sensors in a cost-effective and large-scale way is in high demand in practical wearable applications. Moreover, for clothing purpose, other performances such as light weight, waterproofness, breathability, and thermal management should also be considered [20].

Here, we introduce a general strategy to fabricate flexible tactile sensors for which the textile (or other porous material) itself is the sensing unit through ionic activation. The commercial textile or synthesized porous film could be activated by loading with ionic liquid (IL) on the fabric skeleton, thus constructing EDL capacitive interface when coated with silver nanowires (AgNWs) or flexible silver paste on the substrate. The porous skeleton acts as an elastic structure that allows for fast response, similar to the role of cross-linked macromolecules (or elastomer) in ionic gel. On the other hand, the IL offers the migratory ions in the interface of electrodes and porous substrate to acquire EDL capacitance. Such a method is general: it can be applied to many other daily used materials, such as printing paper sheets, to acquire substantial improvements in sensitivity. We have successfully achieved wearable sensing textiles with a high sensitivity, a fast response time comparable with that of human skin, and high stability over cyclic bends, and that also demonstrated the potential in the applications of health monitoring and motion detection.

2. Results and discussion

Specifically, as illustrated in Fig. 1a, the activation of commercial textile or porous film for constructing flexible tactile sensor was performed by simply immersing the targeted porous material into the IL (1-butyl-3-methylimidazolium hexafluorophosphate, $[BMIM]\cdot PF_6$)/ethanol dispersion, followed by drying to achieve an activated sensing textile in which the IL was loaded onto the skeleton of the porous substrates. The experimental details are provided in the experiment section of Supporting Information. The structure of IL-activated sensing textile is similar to that of ionic gel, a cross-linked network matrix with molecular scale tunnels that fill IL, as illustrated in Fig. 1b. Here, our IL-activated porous materials behave in a similar way: the porous skeleton, which is at a micro-millimeter or submillimeter scale, acts as an elastic material that responds to the external force, whereas the loaded IL generates electronic signals by forming an EDL (Fig. 1c). Because of the large capillary force at microscale, the pores or air gaps of textile can be easily infiltrated with IL spontaneously and remain stable after drying. When taking porous cellulose acetate (CA) films as the selected substrate, we can observe that the nanopores were loaded with a thin layer of IL on the walls, evidenced from the scanning electron microscopy image in Fig. 1d. This process presents two advantages over ionic gels. First, ionic gels show limited response speed because of the high viscoelasticity unless surface microstructures are fabricated, which come at a price. The response speed of the IL-activated material, however, is mainly determined by the porous skeleton and can be extremely fast with selection of proper materials. Second, this simple process can be applied for the cost-effective and large-scale fabrication of a variety of porous structures, including commercial textile, for which the textile itself is sensible.

A capacitive-type tactile sensor is constructed by coating AgNWs or flexible silver paste on both sides of the IL-activated textile. The porous structure has a change in geometry under external force to offer a sensitive interfacial contact area in response to pressure. The activated textile here served as a dielectric layer to form an EDL interface between the IL and electrodes. A simple model is illustrated in Fig. 1e to better understand the sensing principle. Unlike the traditional capacitive sensor, the capacitance changes of the ionic interfacial sensor mainly depend on the changes of interfacial contact area between the IL loaded on the porous skeleton and two electrodes [14,21,22]. Under external pressure, the deformation of the porous structure results in increased contact area between the IL and electrodes, thus leading to a variation in interfacial EDL capacitance. Because the initial connect area of the interface is very small owing to the featured porous structure, it is easy to create a larger connect area, resulting in high pressure-capacitance sensitivity.

One of the advantages of using this facile method is that we are able to activate the commercial and daily wearing cloth to achieve the sensing purpose in a specified area. We constructed a sensing area on an arm sleeve around the wrist area, as shown in Fig. 2b, to demonstrate the activated sensing function of the commercial textile. Biocompatible and soft sliver paste was selected as the working electrodes and coated on both sides of the activated area (see the schematic in Fig. 2a). The silver paste could be patterned to various desired shapes such as the SUS-Tech logo, which is much meaningful once considered for the commercial purpose. Fig. 2b shows that the sensing area is highly sensitive to realize the real-time radial artery pulse signal detection (see the real-time recorded video in Supporting Information), indicating that the sensing function could be easily achieved by integrating the IL and flexible electrodes in the activated area in commercial cloth.

Supplementary data related to this article can be found online at https://doi.org/10.1016/j.mtphys.2019.02.002.

In addition, the sensing property achieved by IL activation is a general method which can be extended to many porous structures to construct flexible tactile sensors. We chose four typical substrates including printing paper, textile, porous CA film, and polyester foam to evaluate the activating effect of IL on the sensing performance, such as pressure-to-capacitance sensitivity. We summarized the calculated sensitivity of four typical porous substrates of CA film, printing paper, textile, and foam before and after IL activation in Fig. 2c (details are illustrated in Fig. S1). The sensitivity (S) is defined as $\delta(\Delta C/C_0)/\delta P$, where C_0 is the initial capacitance, ΔC is the relative change of capacitance (C-C_0), and P is the applied pressure [13,16]. It is obvious that the sensitivity was remarkably improved for each substrate after loading with IL in either low-pressure range (0–0.5 kPa) or high-pressure range (0.5–70 kPa). Even for the activated daily used printing paper, the sensitivity could be improved to 1.39 kPa^{-1}, which is higher than that of many specially designed e-skins and ensures precise sensing capacity to detect sporting or health monitoring applications [23]. Meanwhile, for the activated substrates with high porosity such as polyester foam, the maximum sensitivity was achieved up to 14.6 kPa^{-1} in the pressure range of 10–30 kPa, higher than that of most reported capacitive-type tactile sensors based on porous [24,25] or fabric textile [26] structures. It is worth pointing out that all activated substrates studied here could achieve a linear sensing pressure regime of more than 10 kPa, enabling for a wide range of sensing applications [27]. The results prove that our method is a

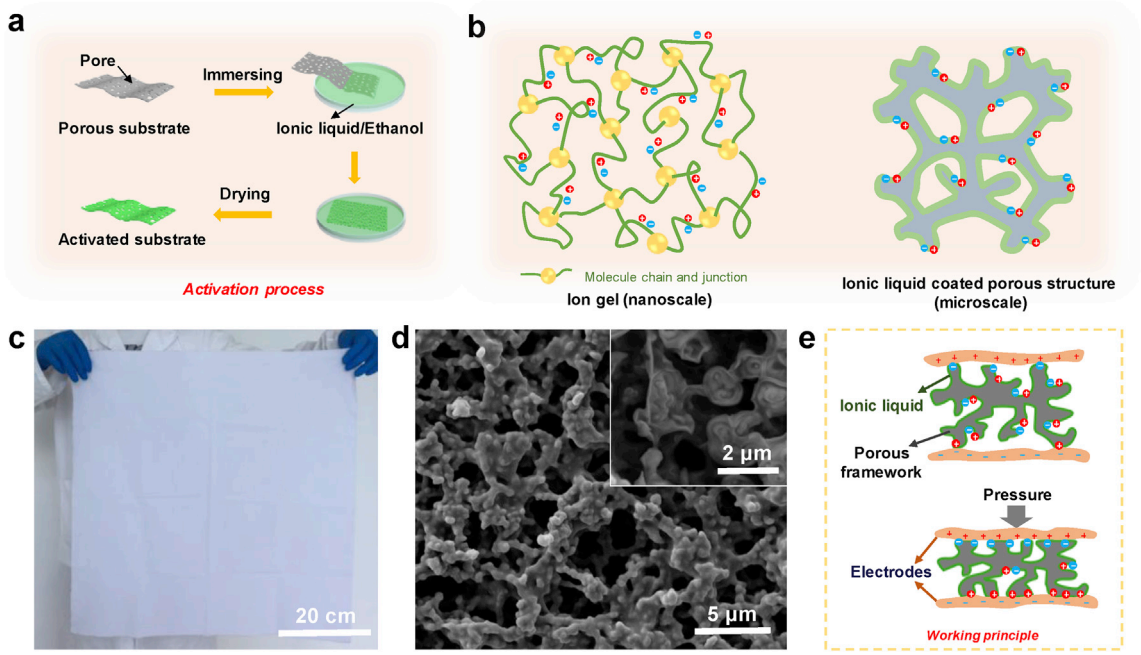

Fig. 1. Sensing mechanism. (a) Schematic illustration of the fabrication process for activating the textile or porous film using ionic liquid. (b) Schematic illustration of ion gel and an ionic liquid-coated porous structure, showing the similar characteristic in nanoscale and microscale. The molecule junctions and porous skeleton are responsible for the mechanical forming, and ions work for the electric performance. (c) The digital photo of a cotton textile loaded with ionic liquid. (d) The morphology of porous cellulose acetate film loaded with ~50 wt% ionic liquid from the surface view and the cross-sectional view (inset). (e) Schematic working principle of an electric double layer interfacial pressure sensor in which the contact area between the porous dielectric layer and electrodes is changed under external mechanical stimuli.

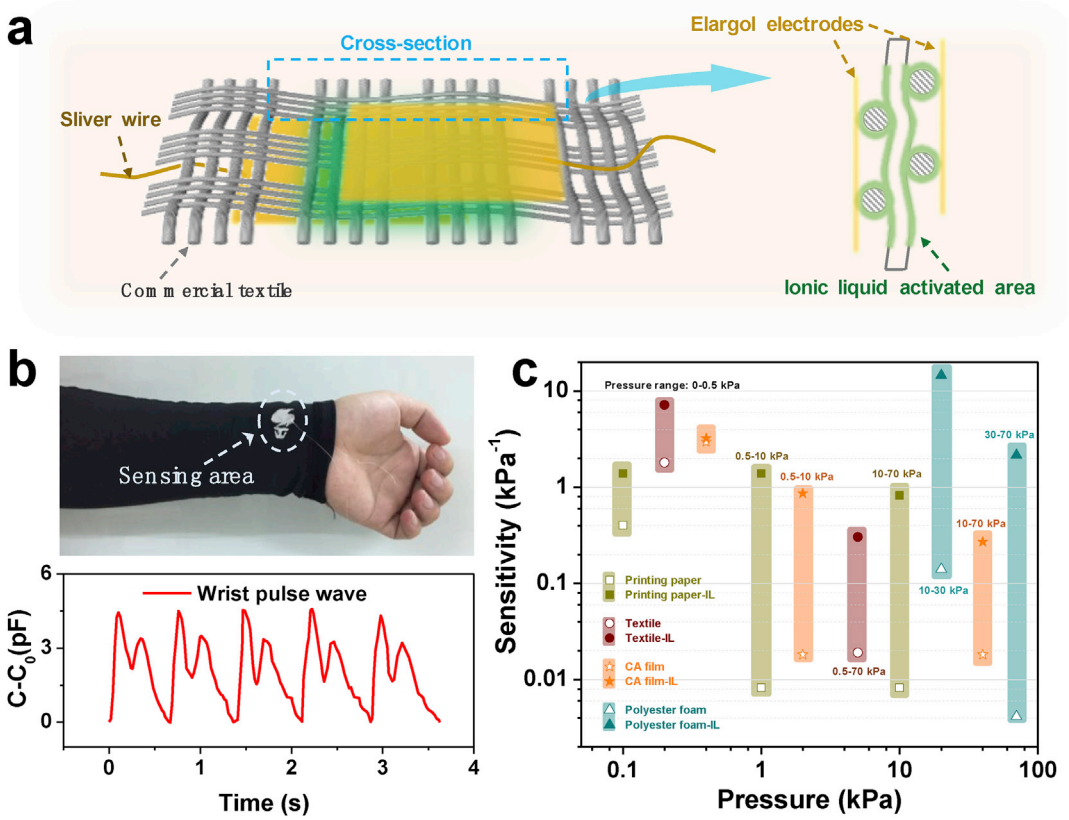

Fig. 2. IL-activated porous materials for pressure sensing. (a) Schematic illustration of the structure of the cloth coupled with a sensing unit, which includes a porous structure activated by IL and biocompatible elargol as electrodes. (b) The radial arterial pulse waveform detected non-invasively on the wrist from an IL-activated commercial tight arm sleeve. (c) The sensitivity of four typical porous materials including printing paper, textile, cellulose acetate (CA) film, and polyester foam before (hollow symbols) and after (solid symbols) coating with IL on the pore wall under different pressure ranges. IL, ionic liquid.

general strategy that can be easily applied to many other material systems with high porosity and low cost. Taking the porous CA film as an example, the activation is estimated to cost only ~3.5 dollar per square meter (~$3.5/m^2, see the details in Supporting Information).

We selected a porous CA film as the substrate to construct a flexible and wearable sensor to further investigate the basic sensing properties and applications because of its more sensitive response under low and middle pressure ranges (0–10 kPa). In addition, the remained porosity of the IL-activated CA film allows for high air permeability, which potentially realizes a breathable interface with human skin for long-term wearing in demand for smart cloth [17]. The flexible sensor was constructed by integrating the IL-activated CA film and cotton textile coated with AgNWs as the electrodes, as illustrated in Fig. S2. The cotton textile was functionalized with superhydrophobic surfaces (the measurements of contact angle presented in Fig. S3) to achieve extended properties such as waterproof and antibacterial ability for long-term clothing purpose [28].

Fig. 3 shows the basic sensing performances of the assembled flexible sensor. The capacitance responses to different pressures applied on the sensor were measured from 0 to 120 kPa with a loading speed of 2 mm/min. The change ratio of capacitance as a function of applied pressure is shown in Fig. 3a. The sensitivities for the sensor are 4.46 kPa^{-1} below the pressure of 0.5 kPa, 0.312 kPa^{-1} under the pressure range of 0.5–10 kPa, and 0.0143 kPa^{-1} under the pressure range of 10–120 kPa. Then, a cup lid that causes an applied pressure of 30 Pa was carefully loaded on the surface of the sensor to investigate the response speed, and it shows that the capacitance of the sensor rapidly ascended within 39 ms, as shown in Fig. 3b, which is comparable with the response speed of human skin (30–50 ms) [29]. The fast response speed lies in the elastic feature of the CA film.

The flexibility of the sensor is important to its applications. Thus, we investigated the capacitance change of the sensor at different deformation modes including twisting and bending. Fig. 3c shows the capacitance response on twisting the sensor up to 360° and recovering it to the initial state. It shows that the sensor exhibits

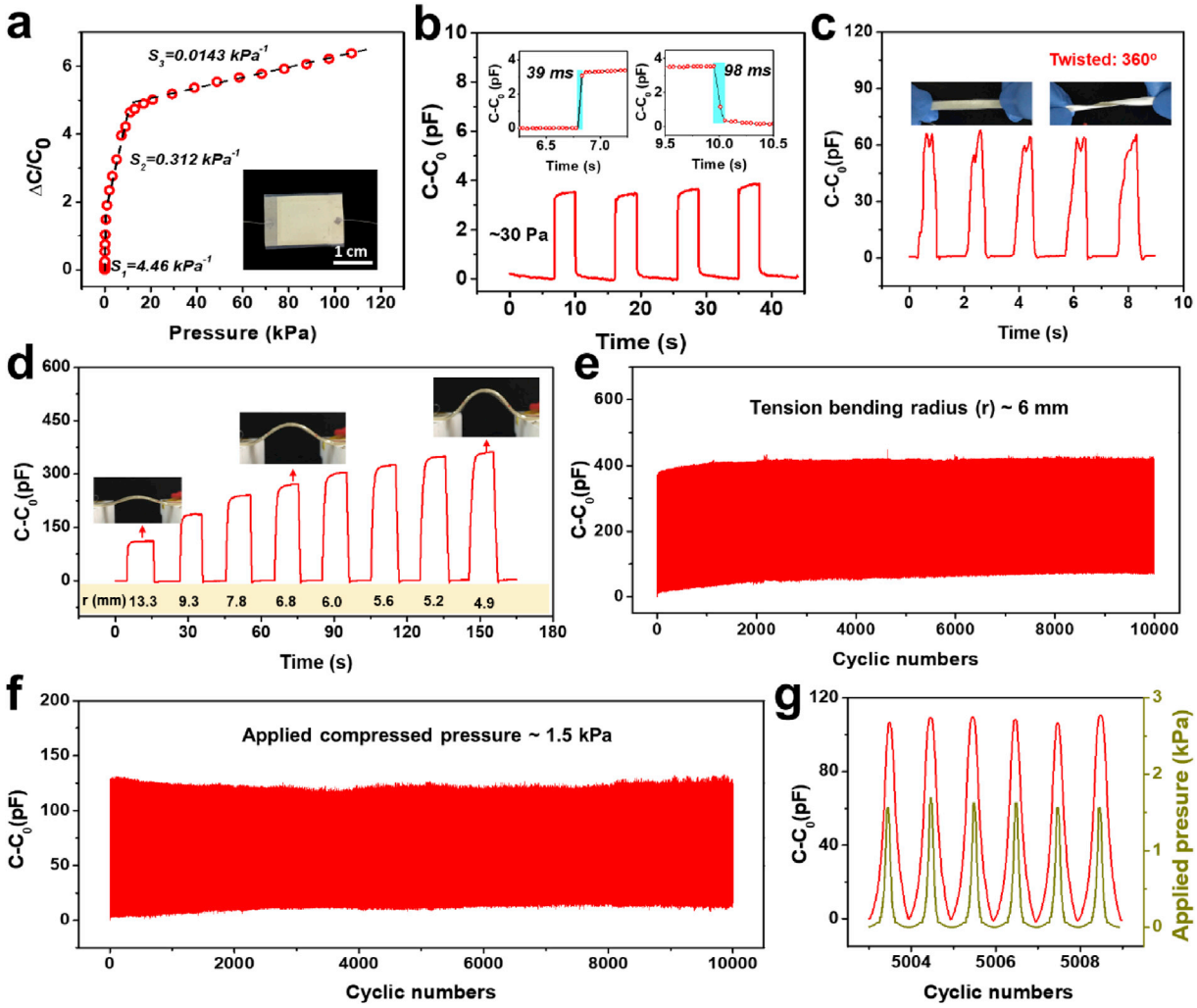

Fig. 3. Sensing properties and flexibility of the IL-activated CA film–based sensor. (a) The capacitance changes of the flexible sensor as a function of pressure under the pressure regime less than 120 kPa. The inset shows an assembled device. (b) Response time of the sensor to a cap (~30 Pa) placed on the top surface of the sensor. The inset shows the time-resolved capacitance change under the loaded and released state. (c) Real-time capacitance changes while twisting the sensor up to 360°. (d) The capacitance changes of the sensor integrated on the multifunctional cloth under various tension bending radii. The insets are photos of the bent sensor under radii of 13.3 mm, 6.8 mm, and 4.9 mm. (e) The working stability of the sensor over 10,000 cycles under a convex bending radius of 6 mm and the capacitance change with the bending deformation around 8000 cycles. (f) and (g) The working stability of the sensor for 10,000 cycles under repeated loading and unloading at a compressive pressure of 1.5 kPa and the capacitance change with the loading around 5000 cycles. CA, cellulose acetate; IL, ionic liquid.

noise-free and highly reproducible signals under continuous twisting force, suggesting high twisting stability. For static bending test, the sensor reflects to a sensitive increase in capacitance as the bending radius decreases, as shown in Fig. 3d, thereupon returning to the initial value when the device goes to the non-bent status. Considering that the wearable sensors inevitably suffer from complicated and long-term loadings, we evaluated the stability and mechanical durability of the sensor by applying cyclic bending (radius, 6 mm) and pressing (1.5 kPa). As shown in Fig. 3e and f, the capacitance changes of the sensor show negligible variation after either repeated bending or pressing over 10,000 cycles, further confirming its high mechanical stability and durability. The capacitance responses and applied pressure waveforms matched well after 5000 cycles of loading/unloading, as shown in Fig. 3g.

The sensor exhibits outstanding sensing performances including high sensitivity, fast response, and high stability. The sensing effect is attributed to the interfacial area that changes on loading, producing a corresponding capacitive change in the EDL interface to evolve an ionic-type signal. The ionic sensor features a frequency response (Fig. S4), but shows relatively stable signal under different temperatures (23.4, 30.2, and 40.9 °C) or relative humidities (30%, 67%, and 95%) (Fig. S5) [14,30]. The response of capacitance to pressure shows hysteresis feature (Fig. S6), probably because of the viscosity of the IL. The high sensitivity is related to the small contact area before loading as a smaller initial area would lead to a larger change in area on pressing to achieve high pressure-capacitance sensitivity. As illustrated in Fig. S7 in Supporting Information, the sensitivity under the pressure range of 0.5–10 kPa is not improved with the increased loading of IL. This has been confirmed by the scanning electron microscope (SEM) images in Fig. S8 in Supporting Information, which shows that a higher loading capacity of IL will further fill the pores up, resulting in a small area fraction to increase under pressure. Although the IL is not sealed in the porous CA film, it does not leak when loaded at high pressures (up to 70 kPa) or subjected to 10,000 cycles of bending or compression. The stable trapping effect of the IL might be attributed to the nanoscale pores. Typically, at nanoscale, the capillary force can generate pressure from the MPa to GPa level [31], which is strong enough to trap the liquid, either in an unloading or under a loading state.

Based on the advantageous features of high sensitivity, our sensor could be applied to detect various vibrations produced correspondingly from different activities and the inherently physiological signals as well. To demonstrate the potential of applications, we assembled the flexible sensor to different positions on a human body to evaluate whether vibration signals could be detected accurately. As illustrated in the photos and schematic in Fig. 4a, the sensing unit was positioned on the wrist and chest near the heart for real-time monitoring of physiological signals, such as pulse, breathing, and heartbeats, and also attached on the elbow joint, knee joint, front sole, and heel to monitor the sporting motions such as elbow and knee joint flexions, walking, and running. It is obvious to see that the signals appeared during breathing at either a slow or fast rate (Fig. 4b), along with the clear fluctuations in the valley of breathing signals, which are reasonably assigned to the variations of heartbeat (Fig. 4c). The high sensitivity of the sensor should be responsible to identify such weak variations. Fig. 4d shows a set of radial artery pressure waves in normal condition and after doing exercise, in which a different pulse rate can be evidently seen. Because of the high resolution provided by the high sensitivity of the sensor, more additional details could be obtained from a typical pulse waveform (Fig. 4e), which shows two distinct peaks (P_1 and P_2) caused by superposition of the incoming blood wave ejected by the left ventricle and the reflected wave from the lower body [32]. For the participant (30 years old, 172 cm, and 60 kg), the radial augmentation index AI_r determined from the waveform, defined as P_2/P_1 [5], is about 69%, a characteristic value expected for a healthy adult male.

Fig. 4f presents the sensing performance of the elbow joint flexions. The capacitance change is detected evidently depending on the bending degree of the elbow joint. The responded signals are repeated well when bending the elbow joint over cycles and remain at the initial value while the elbow returns back to the start point. We have also measured the motion of the knee joint during flexion, as shown in Fig. 4g. The capacitance increases rapidly accompanied by flexing the knee joint and then drops sharply because of the knee extension. In addition, we attached our sensor to the front sole and heel of the feet simultaneously to evaluate the forcing situation when walking or running. As seen in Fig. 4h, a clear signal with sharp tips at the beginning was detected when forcing the front sole and then recovered to the initial value by uplifting the front sole. The capacitance increases accordingly when turning to the load on the heel (Fig. 4i). Note that the capacitance change generated by running is less than that generated by walking, which is in contradiction with our common sense, and the result is probably caused by the uncontacted small forcing area while running. Unlike the commercial step counter based on the gyroscope and localizer in the commercial device, such a capacitive sensor is able to achieve the real stepping information, which may enable potential applications in sporting management. Furthermore, for repeated elbow and knee flexing, running, and walking, the capacitance evolutions for each motion were kept in the same tendency regularly, suggesting that those motions can be identified by determining the characteristic signal using our sensor.

Considering the long-term motions detecting of wearable sensors, the comfort performances such as breathability, waterproofness, and washability are highly demanded, especially for clothing purpose. However, the electrodes and dielectric layer for most wearable capacitive sensors consist of solid materials [33], which are often not breathable. In contrast, our sensor is based on a CA film or cotton textile, both features with a porous structure and exhibits excellent air or sweat permeability, as shown in Fig. S9. The gas permeability is assessed by measuring the mass increase of the desiccant in a glass bottle sealed by the IL-activated CA film supported on the cotton textile, and the moisture permeation is 0.929 $mg/cm^2 \cdot hr$, with a negligible change of weight gain rate of only 6% compared with that of the normal cotton. Such high breathability should be ascribed to the high porosity remained in IL-activated CA film (Fig. S2) and the porous nature of the woven textile (Fig. S10). These pores were not blocked because the length of the AgNWs (100 μm long) is far larger than the diameter of the original pores (~3 μm) of the CA film. Moreover, the signals are still clear enough to identify the characteristics of breathing and heartbeats after several cycles of dry cleaning (Fig. S11). The resistance of two connected AgNW-coated electrodes changes under a small range (30% increased after seven cleaning cycles, Fig. S12), which can hardly affect the performance of the capacitive device. Even for the perspiration-wetted sensor, the sensor could still exhibit a similar signal waveform but with higher capacitance amplitude because of the ionic feature of human perspiration (Fig. S13). Note that for wearable sensors, the amplitude of signals is often not important. Therefore, these additional functions could ensure comfortable feeling while wearing with the aid of high porosity that enables air or sweat to permeate through the whole sensing area during sporting, thus being reusable for long-term applications.

Furthermore, the IL-activated process for fabricating a flexible sensor offers a general way to construct a sensing unit on desired substrates, as presented in this work. It is also expected to extend more functions to the sensing textile considering clothing purpose

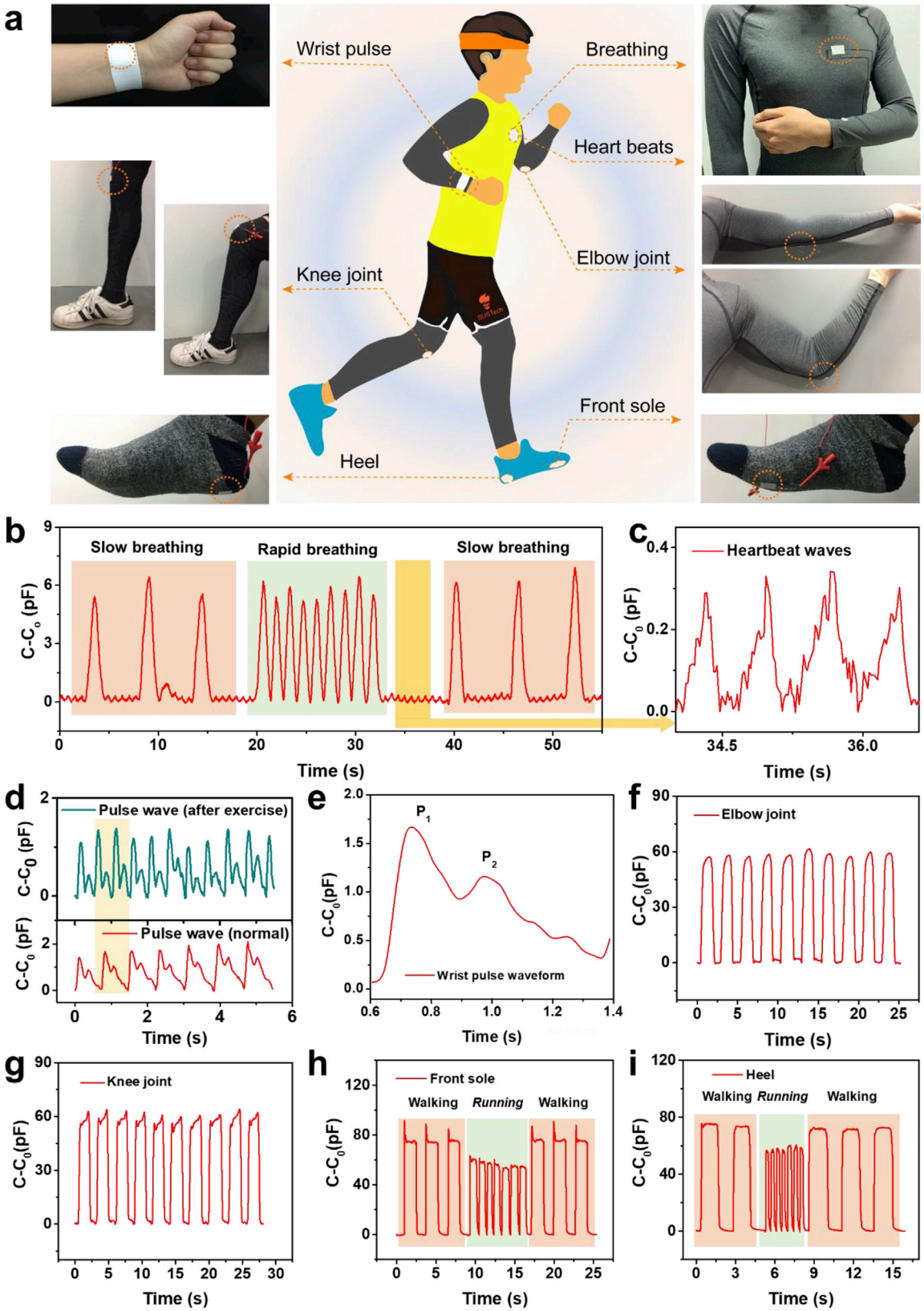

Fig. 4. IL-activated sensor as wearable physiological signal and motion monitoring. (a) Schematic illustration and photographs of positions assembled on the human body for physiological signals and various human motions using the porous CA film–based sensor. (b) Capacitive signals of slow and rapid breathing using the flexible sensor attached to the chest near the heart, clearly showing the heartbeat wave simultaneously in panel (c). (d) Pulse wave signals of the radial artery under normal condition and after doing exercise states measured with the flexible sensor. (e) A single pulse waveform at a normal rate, for calculating the radial augmentation index AI_r. (f) and (g) Signals of the bending elbow joint and knee joint. (h) and (i) Signals of walking and running measured with the sensor attached to the front sole and heel. CA, cellulose acetate; IL, ionic liquid.

such as outdoor performance and long-term hygiene. Therefore, we selected a functionalized cotton textile with a superhydrophobic surface to achieve waterproof and self-cleaning functions by removing the contaminating particles through impacting and/or rolling water droplets (as demonstrated in Fig. S14). Besides, the flexible sensor also exhibits antibacterial property because of the effective antibacterial ability of AgNWs, as shown in Fig. S15. An empty gap around the device placed in a petri dish reveals its ability to suppress the growth of bacteria. The self-cleaning and antibacterial properties enable the sensor to create a healthy internal environment and clean external ambient when sensing the motions and physiological signals.

3. Conclusions

In summary, we introduced a versatile, saleable, and easy operating approach to fabricate flexible sensors by simply activating textile or porous films with IL and constructing an EDL capacitive interface by further coating with flexible electrodes. Such a method enables the sensing elements to be localized on desired areas, allowing for the customization of the sensing unit with a desired pattern on the textile or commercial cloth. Even the daily used materials such as printing paper can be activated as the dielectric layer in tactile sensors that show a sensitivity of more than 1 kPa^{-1}. By integrating the IL-activated porous CA film and cotton textile, the flexible sensor provides a maximum sensitivity of 4.46 kPa^{-1}, a fast response time (~39 ms), and mechanical stability under harsh deformations (10,000 cycles of bending or compression). These sensing performances allow the textile to detect various human motions of sporting or normal movements and also enable to monitor the biomechanical signals such as breathing, heartbeat, and pulse waveform. In addition, the sensor can be breathable, waterproof, washable, and antibacterial for desired clothing purpose, offering high comfort for long-term wearing. The activation of porous films or textiles with IL is a general strategy for large-scale and cost-effective manufacturing of highly sensitive sensors for motion and physiological signal monitoring and other applications. We believe such an approach offers a general strategy to make high-performance wearable electronics to realize the practical applications once integrated with data collecting and launching units, which would be focused on in a further work.

4. Experimental section

Materials

A commercially available cotton textile and CA film were used as the substrate. The IL, 1-butyl-3-methylimidazolium hexafluorophosphate ([BMIM]·PF_6), was obtained from the Lanzhou Institute of Chemical Physics, China. The AgNWs with a diameter of ~50 nm and a length of ~100 μm were obtained from Nanjing XFNANO Materials Tech Co., Ltd.

Fabrication of the flexible sensor

The AgNWs were spray coated on the surface of the functional cotton relative to the waterproof side. After that, a silver wire was mounted to connect AgNWs, which acts as the top electrode. Subsequently, the CA film was immersed into the IL ([BMIM]·PF_6) solution of absolute ethyl alcohol with the weight ratio of 1:1. The unfixed IL was washed away from the porous skeleton by using deionized water through vacuum filtration, and the porous skeleton was dried to obtain the CA-IL film with 50 wt% loading of IL. After that, the AgNWs were spray coated on the surface of the CA-IL film, which acts as the bottom electrode. Finally, the functional cotton was laminated on the CA-IL film, and the edges were bonded together using a 3 M Scotch tape to assemble the multifunctional cloth integrated with the sensing unit as the flexible sensor. For the twisting and bending test samples, the assembled sizes of the obtained sensing textile are 1′3 cm^2 and 1′1 cm^2 with the thickness of ~1 mm.

Characterizations

The sensing performances of the multifunctional cloth were dynamically tested using a force gauge with a computer-controlled stage (XLD-20E, Jingkong Mechanical Testing Co., Ltd) and a capacitance meter (LCR meter, E4980AL, Keysight). The capacitance changes were recorded in real-time using LabVIEW software with a frequency of 10^5 Hz. The mechanical durability of the sensing textile was evaluated using a step motor (WS150-100).

Conflicts of interest

The authors declare no competing interests.

Acknowledgments

This work was financially supported by the funds of the National Natural Science Foundation of China (no. 51771089 and U1613204), 'Guangdong Innovative and Entrepreneurial Research Team Program' under contract no. 2016ZT06G587, Shenzhen DRC project [2018]1433, 'Science Technology and Innovation Committee of Shenzhen Municipality' (grant no. JCYJ20170817111714314 and JCYJ20160613160524999), and 'Peacock Plan' (no. Y01256120). M. G. also thanks the support of 'College Student's Innovation and Entrepreneurship Program' (no. 2018X33).

Appendix A. Supplementary data

Supplementary data to this article can be found online at https://doi.org/10.1016/j.mtphys.2019.02.002.

References

[1] L. Van Langenhove, C. Hertleer, Int. J. Cloth Sci. Technol. 16 (1/2) (2004) 63.
[2] W. Zeng, L. Shu, Q. Li, S. Chen, F. Wang, X.M. Tao, Adv. Mater. 26 (31) (2014) 5310.
[3] C.-C. Yang, Y.-L. Hsu, Sensors 10 (8) (2010) 7772.
[4] H. Yu, S. Cang, Y. Wang, A review of sensor selection, sensor devices and sensor deployment for wearable sensor-based human activity recognition systems, in: IEEE 2016 10th International Conference on Software, Knowledge, Information Management & Applications (SKIMA), IEEE, Chengdu, China, 2016, p. 250.
[5] G. Schwartz, B.C. Tee, J. Mei, A.L. Appleton, D.H. Kim, H. Wang, Z. Bao, Nat. Commun. 4 (5) (2013) 1859.
[6] Y. Wan, Y. Wang, C.F. Guo, Mater. Today Phys. 1 (2017) 61.
[7] R. Bao, C. Wang, L. Dong, R. Yu, K. Zhao, Z.L. Wang, C. Pan, Adv. Funct. Mater. 25 (19) (2015) 2884.
[8] H. Gullapalli, V.S. Vemuru, A. Kumar, A. Botello-Mendez, R. Vajtai, M. Terrones, S. Nagarajaiah, P.M. Ajayan, Small 6 (15) (2010) 1641.
[9] A. Proto, M. Penhaker, D. Bibbo, D. Vala, S. Conforto, M. Schmid, Sensors 16 (4) (2016) 524.
[10] S. Gong, W. Schwalb, Y. Wang, Y. Chen, Y. Tang, J. Si, B. Shirinzadeh, W. Cheng, Nat. Commun. 5 (2014) 3132.
[11] Y. Wang, L. Wang, T. Yang, X. Li, X. Zang, M. Zhu, K. Wang, D. Wu, H. Zhu, Adv. Funct. Mater. 24 (29) (2014) 4666.
[12] S.J. Kim, W. Song, Y. Yi, B.K. Min, S. Mondal, K.-S. An, C.-G. Choi, ACS Appl. Mat. Interfaces 10 (4) (2018) 3921.
[13] Y. Wan, Z. Qiu, Y. Hong, Y. Wang, J. Zhang, Q. Liu, Z. Wu, C.F. Guo, Adv. Electron. Mater. (2018) 1700586.
[14] R. Li, S. Yang, Z. Zhu, Y. Guo, Y. Zhang, N. Pan, G. Sun, T. Pan, Adv. Mater. 29 (36) (2017) 1700253.
[15] B. Nie, S. Xing, J.D. Brandt, T. Pan, Lab Chip 12 (6) (2012) 1110.
[16] Z. Qiu, Y. Wan, W. Zhou, J. Yang, J. Yang, J. Huang, J. Zhang, Q. Liu, S. Huang, N. Bai, Adv. Funct. Mater. (2018) 1802343.

[17] J.S. Heo, J. Eom, Y.H. Kim, S.K. Park, Small 14 (3) (2018) 1703034.
[18] K. Sim, Y. Gao, Z. Chen, J. Song, C. Yu, Adv. Mater. Technol. (2018) 1800466.
[19] Y. Gao, K. Sim, S. Sun, Z. Chen, J. Song, C. Yu, IEEE Trans. Compon. Packag. Manuf. Technol. 5 (9) (2015) 1230.
[20] M. Stoppa, A. Chiolerio, Sensors 14 (7) (2014) 11957.
[21] B. Nie, R. Li, J.D. Brandt, T. Pan, Lab Chip 14 (6) (2014) 1107.
[22] K.H. Lee, M.S. Kang, S. Zhang, Y. Gu, T.P. Lodge, C.D. Frisbie, Adv. Mater. 24 (32) (2012) 4457.
[23] Y. Zang, F. Zhang, C.-a. Di, D. Zhu, Mater. Horiz. 2 (2) (2015) 140.
[24] O. Atalay, A. Atalay, J. Gafford, C. Walsh, Adv. Mater. Technol. 3 (1) (2018) 1700237.
[25] D. Kwon, T.-I. Lee, J. Shim, S. Ryu, M.S. Kim, S. Kim, T.-S. Kim, I. Park, ACS Appl. Mat. Interfaces 8 (26) (2016) 16922.
[26] J. Lee, H. Kwon, J. Seo, S. Shin, J.H. Koo, C. Pang, S. Son, J.H. Kim, Y.H. Jang, D.E. Kim, Adv. Mater. 27 (15) (2015) 2433.
[27] Y. Shu, H. Tian, Y. Yang, C. Li, Y. Cui, W. Mi, Y. Li, Z. Wang, N. Deng, B. Peng, Nanoscale 7 (18) (2015) 8636.
[28] Q. Liu, J. Huang, J. Zhang, Y. Hong, Y. Wan, Q. Wang, M. Gong, Z. Wu, C.F. Guo, ACS Appl. Mat. Interfaces 10 (2) (2018) 2026.
[29] A. Chortos, Z. Bao, Mater. Today 17 (7) (2014) 321.
[30] Z. Wen, M.-H. Yeh, H. Guo, J. Wang, Y. Zi, W. Xu, J. Deng, L. Zhu, X. Wang, C. Hu, Sci. Adv. 2 (10) (2016) e1600097.
[31] Y. Liu, J. Zhang, H. Gao, Y. Wang, Q. Liu, S. Huang, C.F. Guo, Z. Ren, Nano Lett. 17 (2) (2017) 1090.
[32] W.W. Nichols, Am. J. Hypertens. 18 (S1) (2005) 3S.
[33] S.C. Mukhopadhyay, IEEE Sens. J. 15 (3) (2015) 1321.